Comparative Genomic Sequence and Expression Analyses of *Medicago truncatula* and Alfalfa Subspecies *falcata COLD-ACCLIMATION-SPECIFIC* Genes[1][W][OA]

Joyce C. Pennycooke, Hongmei Cheng[2], and Eric J. Stockinger*

Department of Horticulture and Crop Science, The Ohio State University/Ohio Agricultural Research and Development Center, Wooster, Ohio 44691

In Arabidopsis (*Arabidopsis thaliana*) the low-temperature induction of genes encoding the C-REPEAT BINDING FACTOR (CBF) transcriptional activators is a key step in cold acclimation. CBFs in turn activate a battery of downstream genes known as the CBF regulon, which collectively act to increase tolerance to low temperatures. Fundamental questions are: What determines the size and scope of the CBF regulon, and is this is a major determinant of the low-temperature tolerance capacity of individual plant species? Here we have begun to address these questions through comparative analyses of *Medicago truncatula* and *Medicago sativa* subsp. *falcata*. *M. truncatula* survived to −4°C but did not cold acclimate, whereas *Medicago falcata* cold acclimated and survived −14°C. Both species possessed low-temperature-induced *CBFs* but differed in the expression of the *COLD-ACCLIMATION-SPECIFIC* (*CAS*) genes, which are candidate CBF targets. *M. falcata CAS30* was robustly cold-responsive whereas the Mt*CAS31* homolog was not. *M. falcata* also possessed additional *CAS30* homologs in comparison to the single *CAS31* gene in *M. truncatula*. Mf*CAS30* possessed multiple pairs of closely spaced C-REPEAT/DEHYDRATION RESPONSIVE ELEMENT (CRT/DRE) motifs, the cognate CBF binding site in its upstream region whereas Mt*CAS31* lacked one CRT/DRE partner of the two proximal partner pairs. *CAS* genes also shared a promoter structure comprising modules proximal and distal to the coding sequence. *CAS15*, highly cold-responsive in both species, harbored numerous CRT/DRE motifs, but only in the distal module. However, fusion of the Mt*CAS15* promoter, including the distal module, to a reporter gene did not result in low-temperature responsiveness in stably transformed Arabidopsis. In contrast, both Mt*CAS31* and Mf*CAS30* promoter fusions were low-temperature responsive, although the Mf*CAS31* fusion was less robust than the Mf*CAS30* fusion. From these studies we conclude that *CAS* genes harbor CRT/DRE motifs, their proximity to one another is likely key to regulatory output in *Medicago*, and they may be located kilobases distal to the transcriptional start site. We hypothesize that these differences in CRT/DRE copy numbers in *CAS30/CAS31* upstream regions combined with differences in gene copy numbers may be a factor in determining differences in low-temperature tolerance between *M. truncatula* and *M. falcata*.

Many plants increase their capacity to survive freezing temperatures after exposure to a period of low, nonfreezing temperatures, a process known as cold acclimation (Thomashow, 1990, 1999). In Arabidopsis (*Arabidopsis thaliana*), a major pathway leading to cold acclimation and freezing tolerance is the C-REPEAT BINDING FACTOR (CBF) response pathway. The CBFs are transcriptional activators that bind to the

C-REPEAT/DEHYDRATION RESPONSIVE ELEMENT (CRT/DRE), which has at its core a 5-bp motif, CCGAC (Stockinger et al., 1997). Initially identified as the DNA regulatory element critical for the low-temperature induction of the *COR* genes (Baker et al., 1994; Yamaguchi-Shinozaki and Shinozaki, 1994; Wang et al., 1995; Iwasaki et al., 1997), the CRT/DRE is now known to effect cis-acting regulatory control over a much larger network of regulatory and structural genes referred to as the CBF regulon (Fowler and Thomashow, 2002; Vogel et al., 2005). The CBF regulon in turn functions to impart freezing tolerance (Jaglo-Ottosen et al., 1998; Liu et al., 1998; Jaglo et al., 2001). Through mechanisms that have only recently begun to be understood (Chinnusamy et al., 2003; Zarka et al., 2003), the CBFs are themselves induced in response to low temperatures, initiating the regulatory cascade (Gilmour et al., 1998).

Tomato (*Solanum lycopersicum*), a chilling sensitive plant also harbors *CBF* genes that respond to low temperatures (Zhang et al., 2004). However, only four of the approximately 8,000 surveyed tomato genes are CBF responsive (Zhang et al., 2004). At least eight additional genes on the 8,000-gene array are orthologs of Arabidopsis CBF-responsive genes harboring CRT/DRE

motifs in their regulatory regions (Zhang et al., 2004). A conclusion from these data is that the tomato CBF regulon is smaller and less diverse than the Arabidopsis CBF regulon (Zhang et al., 2004). These experiments raise important questions as to what determines the size and scope of the CBF regulon. Is it the CRT/DRE, or is it a CBF cofactor required for a CBF to activate genes harboring CRT/DRE motifs? And are differences in the CBF regulon in taxonomically allied plants that differ in their low-temperature tolerance due to differences in the CBF regulon?

In alfalfa (*Medicago sativa*) a freezing-tolerant plant that cold acclimates, transcripts encoding the COLD-ACCLIMATION-SPECIFIC (CAS) proteins are induced and accumulate to very high levels during cold acclimation (Mohapatra et al., 1989; Monroy et al., 1993; Wolfraim and Dhindsa, 1993; Wolfraim et al., 1993). Also known as the *COLD-ACCLIMATION-RESPONSIVE* (*CAR*; Haagenson et al., 2003), *CAS* gene expression levels parallel low-temperature tolerance levels of individual cultivars; higher transcript levels accumulate in genotypes that have greater lower temperature tolerance in comparison to genotypes that have lesser lower temperature tolerance and that exhibit lower and more transient *CAS* expression profiles (Mohapatra et al., 1989). The similarities in expression profiles between Arabidopsis *COR* genes and alfalfa *CAS* genes suggests that the *CAS* genes are under a cis- and trans-regulatory control system homologous to that of the Arabidopsis *COR* genes.

Alfalfa is one of 83 *Medicago* species (Small and Jomphe, 1989). Most are herbaceous plants that either have an annual growth habit in which the plant dies after fruiting, or a perennial growth habit in which the underground portion of the plant survives winter, but the upper portion does not. Alfalfa is of the latter, perennial growth habit type. It is also a complex polymorphic species resulting from domestication, polyploidization, interspecific, and intraspecific hybridization among subspecies groups (Lesins and Lesins, 1979; Quiros and Bauchan, 1988; Small and Jomphe, 1989). Cultivars consist of populations rather than homozygous inbred lines because of inbreeding depression (Jones and Bingham, 1995). In contrast, *Medicago truncatula*, a lesser-grown forage legume, is an annual, diploid, and self-pollinating species. Recently, *M. truncatula* has been established as a model to facilitate molecular genetic analyses of alfalfa and other leguminous plants (Barker et al., 1990; Cook, 1999). Model status has generated a wealth of resources including collections of ecologically adapted genotypes (Cook, 1999), mutants (Penmetsa and Cook, 2000), BAC libraries (Nam et al., 1999), collections of EST sequences (Bell et al., 2001; Lamblin et al., 2003), and soon, the complete genome sequence (Young et al., 2005).

In this study, we compared *M. truncatula* and alfalfa subsp. *falcata*, a diploid subspecies of alfalfa, in their capacity to cold acclimate and in components of the CBF cis-/trans-transcriptional regulatory system. A specific objective was to determine the structure of the

Medicago CAS genes and explore whether they might be under a cis- and trans-regulatory control system homologous to that of the Arabidopsis *COR* genes.

RESULTS

M. truncatula Survives to −4°C But Cold-Acclimating Conditions Do Not Significantly Increase Its Capacity to Survive Freezing

To determine whether *M. truncatula* could cold acclimate and survive freezing, 4-week-old plants of *M. truncatula* and alfalfa subsp. *falcata*, hereafter referred to as *Medicago falcata*, were placed at +2°C for 4 weeks, and then subjected to a series of decreasing temperatures below freezing. *M. truncatula* survived to about −4°C whether plants were subjected to cold-acclimating conditions prior to freezing or not (Fig. 1B). In comparison, *M. falcata* survived to about −6°C
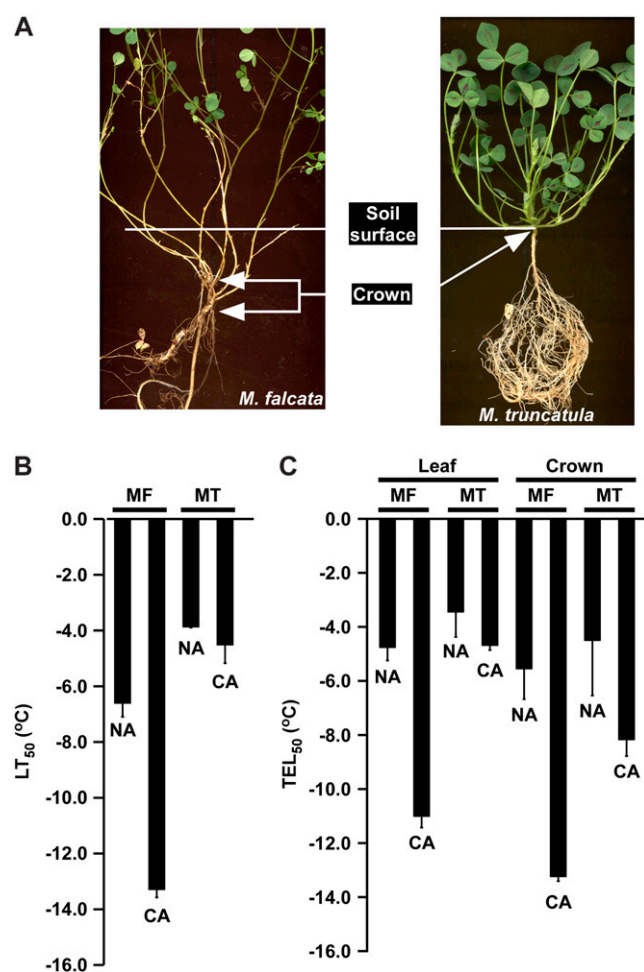
Figure 1. Freezing tolerance of *M. falcata* (MF) and *M. truncatula* (MT) plants after 4 weeks growth at 20°C/18°C day/night (NA), or after an additional 4 weeks at +2°C (CA). A, Crown regions used for electrolyte leakage and whole-plant freezing assays. B, Temperature at which 50% of the plants failed to regrow (LT_{50}) after freezing to the indicated temperatures. C, Temperature at which 50% electrolyte leakage (TEL_{50}) occurred after freezing.

without prior exposure to cold; and survived and regrew after exposure to nearly $-14°C$ when cold acclimated (Fig. 1B). When plants were evaluated by electrolyte leakage, *M. truncatula* had TEL_{50} values of about $-4°C$ whether plants were subjected to cold-acclimating conditions or not. In comparison, leaves from cold acclimated and nonacclimated *M. falcata* yielded TEL_{50} values of $-11°C$, and $-5°C$, respectively (Fig. 1C). Cold-treated *M. truncatula* crown tissues showed a slightly greater TEL_{50} of $-8°C$ (Fig. 1C). These experiments suggest that there is a marginal depression in the temperature at which electrolyte leakage occurs in *M. truncatula* in response to a period of low nonfreezing temperatures, however *M. truncatula* plants are only capable of surviving to $-5°C$, and cold-acclimating conditions do not impart a significantly greater capacity to survive lower temperatures.

M. truncatula and *M. falcata* Differ in Their *CAS* Gene Cold-Responsive Expression

As the CBF transcriptional activators play a central role in the cold-acclimation response of Arabidopsis, we considered that *M. truncatula* and *M. falcata* might differ in one or more components of the CBF response pathway. To explore this idea, three *Medicago CBF* sequences, Mt*CBF1*, Mt*CBF2*, and Mt*CBF3* (based on the chronological order in which they were identified from database searches) alongside *CAS15* and *CAS17* (cold acclimation specific; Mohapatra et al., 1989) probes were used for expression analyses. One hour after decreasing the temperature to 6°C, transcripts cross-hybridizing with Mt*CBF2* and Mt*CBF3* accumulated in both *M. falcata* and *M. truncatula* (Fig. 2A). Transcripts continued to accumulate at 6 and 24 h, albeit transcript abundances were significantly lower at 24 h (Fig. 2A). After seven continuous days at 6°C, transcripts were essentially undetectable (Fig. 2A). Expression analyses using plants subjected to a series of decreasing temperatures indicated that Mt*CBF2* and Mt*CBF3* cross-hybridizing transcripts were detectable in both species at 12°C, 8°C, and 6°C (Fig. 2B). Transcripts cross-hybridizing to Mt*CBF1* were not detected in these experiments at any time point examined in either species (not shown).

In both *Medicago* species, low levels of *CAS15* were detected in warm-grown plants (Fig. 2A). Transcript levels increased in abundance 6 h after decreasing the temperature, and continued to accumulate to very high levels 24 h after the temperature decrease (Fig. 2A). After 7 d, *CAS15* remained elevated in *M. falcata* but was diminished in *M. truncatula* (Fig. 2A). Twenty-four hours after returning plants to 25°C, *CAS15* transcripts decreased to levels detected in the warm-grown plants (Fig. 2A). *CAS17* showed a similar expression profile as *CAS15* in *M. falcata* but was undetectable in *M. truncatula* at a lower RNA loading concentration (Fig. 2A); increasing the amount of RNA loaded onto the gel from 5 to 15 μg allowed for its detection (Fig. 2B). This indicated that very low levels of *CAS17* were
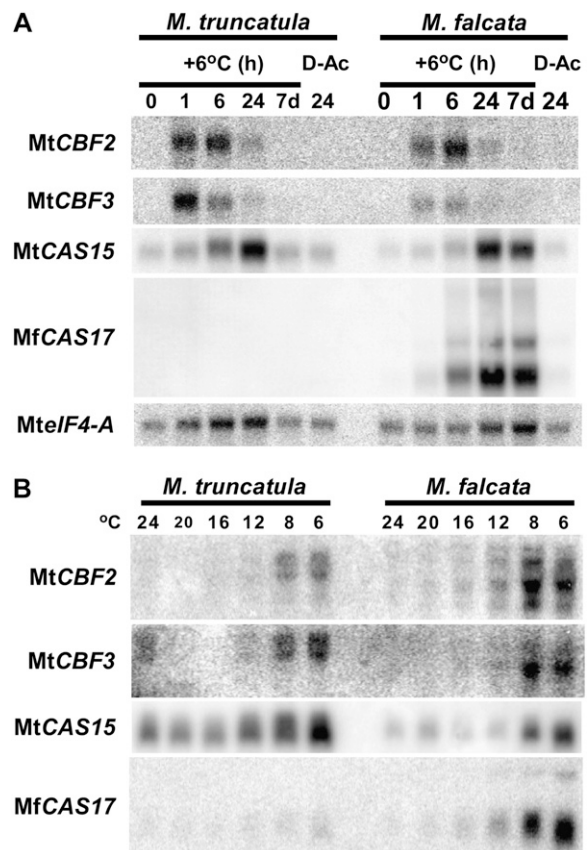

Figure 2. *M. truncatula* and *M. falcata* *CBF* and *CAS* cold-responsive gene expression. A, Time course. Leaf material from plants harvested at 0, 1, 6, and 24 h, and 7 d after the growth chamber temperature equilibrated to 6°C, or 24 h after the chamber was returned to 25°C (D-Ac). Each lane contains 5 μg of total RNA. The same filter was hybridized with each of the indicated probes. B, Temperature step-down series. Leaf material from plants harvested 6 h after decreasing the growth chamber temperature to the indicated temperatures. Each lane contains 15 μg of total RNA.

present in *M. truncatula* at all temperatures, which increased slightly at 12°C and the lower temperatures (Fig. 2B). Faint levels of *CAS17* were also detected at all temperatures in *M. falcata*, and each incremental temperature decrease resulted in *CAS17* levels elevated above the previous temperature, which were most pronounced at 8°C and 6°C (Fig. 2B).

CAS Polypeptide Structure

To determine whether the *Medicago CAS* genes harbored CRT/DRE regulatory motifs, and to explore the mechanism behind the difference in *CAS17* gene expression we sequenced the *M. truncatula* and *M. falcata* *CAS15* and *CAS17* genomic regions using inserts cloned in bacteriophage λ. The *M. truncatula* *CAS15* genomic clone encoded a 13-kD polypeptide, as did the best-hit ESTs to alfalfa *CAS15*, in comparison to the 14.5-kD polypeptide encoded by alfalfa *CAS15* (Fig. 3A). This difference was due primarily to a 15-amino-acid
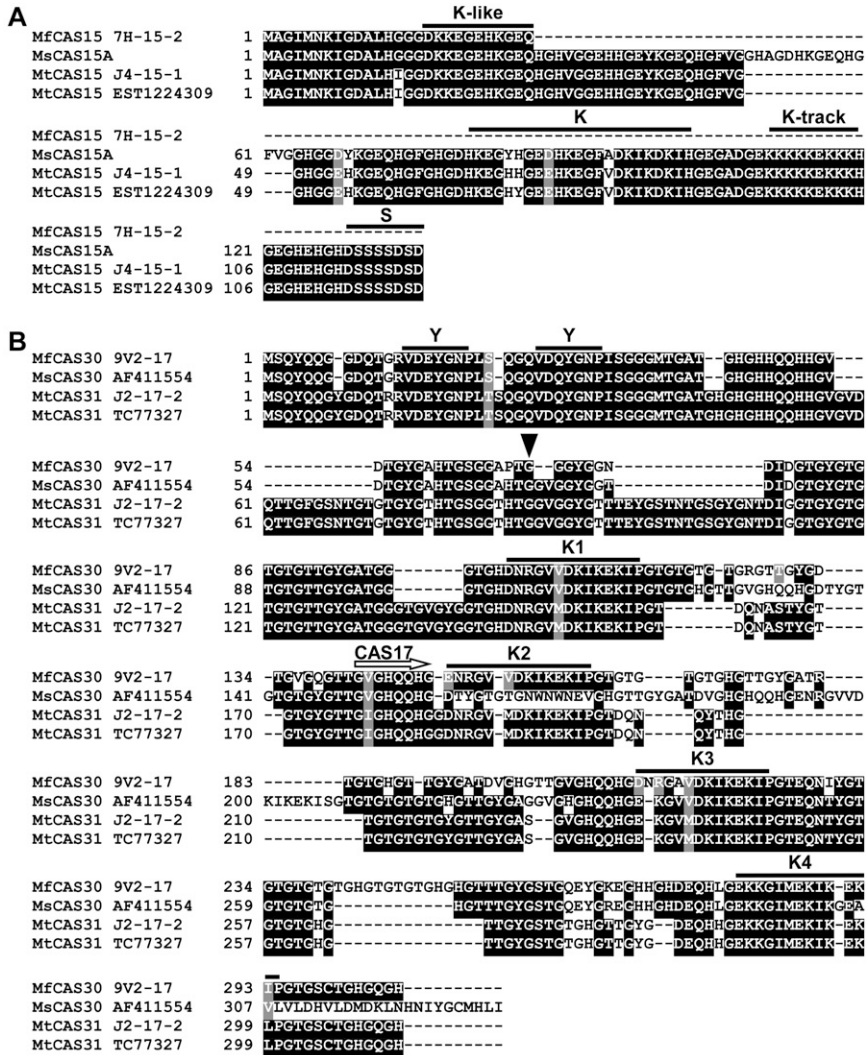
Figure 3. Alignments of polypeptide sequences encoded by *M. truncatula* and *M. falcata* CAS15, CAS30, and CAS31. A, Alignment of predicted CAS15 polypeptides encoded by *M. falcata* λ7H-15-2 (partial length), and *M. truncatula* λJ4-15-1 genomic clones with those encoded by the expressed sequences from alfalfa *CAS15* (GenBank accession L12461; Monroy et al., 1993), and *M. truncatula* EST1224309 (GenBank accession DW015348). B, Alignment of CAS30 and CAS31 polypeptides encoded by *M. falcata* λV2-17 and *M. truncatula* λJ2-17-2 genomic clones with those encoded by alfalfa expressed sequence AF411554 (Ivashuta et al., 2002) and *M. truncatula* TC77327. The downward pointing arrow identifies Gln residues 69 and 89 in *M. falcata* and *M. truncatula* CAS30/31 polypeptides, respectively, whose codon is split between Exons 1 and 2. Sequences were aligned using ClustalX and highlighted using BoxShade. The rightward horizontal arrow indicates where similarity to CAS17 begins. Dehydrin K-, S-, and Y-segments (Close, 1996) are overlined and denoted as such above the sequences. C, Ab initio predicted structure of *M. truncatula* CAS31 and relative positions of sequence assembly TC100921, and EST hits; and the tissue sources for those ESTs. D, RNA blot hybridization under noninducing conditions (W) or after 6 h at 4°C (C) using probes specific to either Mf*CAS30* Exon 1 (E1) or Exon 2/CAS17 (E2).
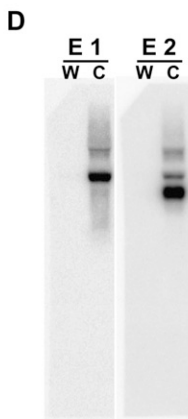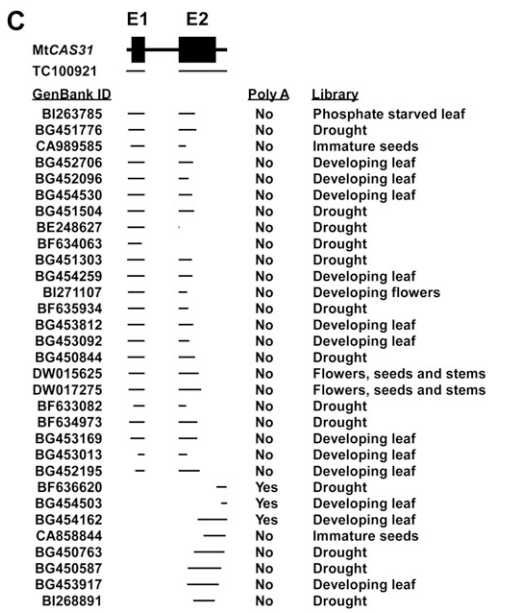
stretch in MsCAS15 that was absent from MtCAS15. Other than the presence versus absence of this stretch, the two polypeptides differed only in five of 136 residues (Fig. 3A). Both MtCAS15 and MsCAS15 possessed the characteristic dehydrin K- and S-segments, a second, shorter motif similar to the K-segment NH_3-terminal to the consensus K-segment, and a nearly homogeneous Lys tract COOH-terminal to the K-segment (Fig. 3A).

Surprisingly, the *M. truncatula* and the *M. falcata* genomic clones isolated with the *CAS17* probe were predicted by ab initio gene structure prediction programs FGENESH and GENSCAN to encode polypeptides much larger than 17 kD. The predicted polypeptide encoded by the *M. truncatula* genomic clone was 31 kD, whereas that of the *M. falcata* genomic clone was 30 kD (Fig. 3B). Similarity to CAS17 started approximately at amino acid residue 140 of the predicted *M. falcata* polypeptide (Fig. 3B). Searches of GenBank and the Gene Index Project databases for expressed sequences encompassing the entire length of these ab initio-predicted genes identified an alfalfa cDNA clone, GenBank accession AF411554 ($E = 1e^{-169}$, score 1,349; Ivashuta et al., 2002), and the *M. truncatula* tentative consensus sequence TC100921 ($E = 7.4e^{-208}$, score 4,695). No single *M. truncatula* EST encompassed the entire predicted coding sequence (CDS; Fig. 3C), however the TC100921 sequence assembly comprising multiple ESTs was 100% identical to the ab initio predicted CDS. RNA blot hybridization using only the upstream part of the predicted CDS indicated that a higher M_r species of RNA cross-hybridized with this probe (Fig. 3D). This higher M_r RNA species also cross-hybridized to the *CAS17* probe; albeit to a lesser degree (Fig. 3D). As these genes likely encoded polypeptides much larger than 17 kD, we designated them Mt*CAS31* and Mf*CAS30*.

At the polypeptide level, MtCAS31 and MfCAS30 each possessed four of the characteristic dehydrin Lys-rich K-segments and a single Y-segment (Fig. 3B). Over the entire length of the polypeptide MtCAS31 and MfCAS30 were about 55% identical. Most of the dissimilarity occurred in the form of small insertions and deletions in the regions between each of these conserved K- and Y-segments (Fig. 3B).

M. truncatula and *M. falcata CAS* Promoters Consist of Proximal and Distal Modules

Alignment of the Mt*CAS15*, Mt*CAS31*, and Mf*CAS30* genomic sequences to their respective expressed sequences revealed that these genes were interrupted by a single intron (Fig. 4A; data not shown). In the instance of Mt*CAS15* the entire protein CDS was contained within Exon 1 (Fig. 4A), whereas Mt*CAS31* and Mf*CAS30* were split between Exon 1 and Exon 2 (Fig. 4B). This single intron in Mt*CAS31* and Mf*CAS30* occurred at a conserved Gly; residue 89 in MtCAS31, and residue 69 in MfCAS30 (Fig. 3B).

Immediately upstream of the *M. falcata* and *M. truncatula CAS15* CDSs was a shared block of nucleotide identity ending at −270 in Mt*CAS15* and −325 in Mf*CAS15* (Fig. 4A; Supplemental Fig. S1). Further upstream, at −1,529 in Mt*CAS15* and −1,819 in Mf*CAS15*, began a second block of nucleotide conservation (Fig. 4A; Supplemental Fig. S1). This second
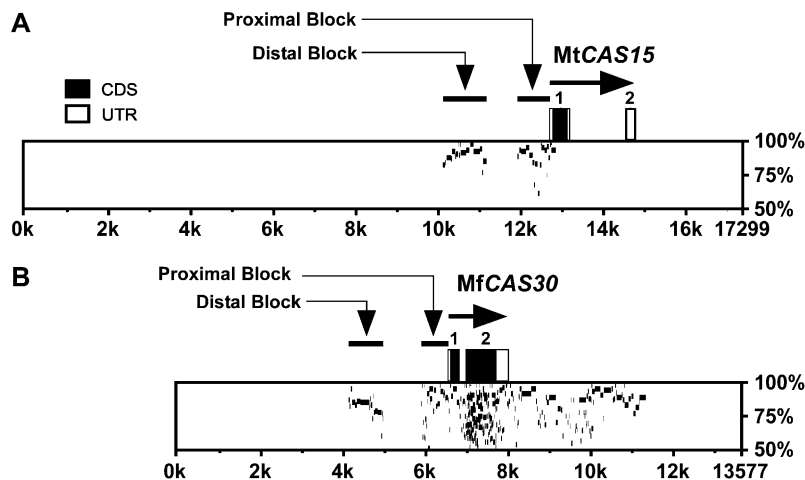

Figure 4. PIPs between the *M. truncatula* and *M. falcata CAS15* and *CAS30/31* genomic regions. A, PIPs between 17,299 bp of the *M. truncatula CAS15* genomic region (horizontal axis) and the 7,779 bp *M. falcata* genomic clone λ7H-15-2 (vertical axis). (The Mf*CAS15* genomic clone λ7H-15-2 terminates at amino acid residue Q27.) B, PIPs between the 13,577 bp *of M. falcata CAS30* genomic clone λV2-17 (horizontal axis) and the 14,288 bp *M. truncatula* λJ2-17-2 genomic clone (vertical axis). The Mt*CAS31* genomic clone λJ2-17-2 terminates at −1,728 within the distal upstream identity block. Exons 1 and 2 are shown as boxes; black boxes are protein CDSs, gray boxes are untranslated regions (UTR). The percent identity between the genomic regions from 50% and 100% is presented on the vertical axis. The multiple horizontal bars at the same position along the *x* axis under Exon 2 in CAS30 are a result of the low complexity and multiple repeating unit structural composition of dehydrins.

block continued to −2,586 of Mt*CAS15* and to −2,807 of Mf*CAS15* (Fig. 4A; Supplemental Fig. S1). Between the two conserved blocks and beyond the second block, the identity between the two genomic regions was negligible (Fig. 4A). In the distal block, five CRT/DRE and two ABRE motifs were present at conserved positions in the two sequences (Supplemental Fig. S1). However, neither *M. falcata* nor *M. truncatula CAS15* harbored CRT/DRE motifs in the proximal block. Because the distal block was more than 1.5 kb upstream of the predicted Met initiator codon, we conducted 5′ RACE experiments to determine if there might be an additional upstream exon, but the data indicated that the transcriptional start site resided 68 bp upstream of the predicted MET initiator codon (Supplemental Fig. S1A).

Alignment of the *M. falcata CAS30* and *M. truncatula CAS31* genomic regions also revealed two blocks of nucleotide identity separated by regions of nonidentity. One block extended to −300 in Mt*CAS31*, and to −313 in Mf*CAS30* (Fig. 4B; Supplemental Fig. S1B). The distal block began at −947 in Mt*CAS31* and −1,611 in Mf*CAS30*, and continued almost to the end of our Mt*CAS31* genomic clone, which corresponded to −1,724 of Mt*CAS31* and −2,383 of Mf*CAS30* (Fig. 4B; Supplemental Fig. S1B). In the Mf*CAS30* proximal conserved block was a pair of CRT/DRE motifs separated by 98 nucleotides and four ABRE motifs (Fig. 5C). The homologous region of Mt*CAS31* harbored these same four ABRE motifs and the most proximal CRT/DRE, but three of the five nucleotides in the second CRT/DRE differed from the consensus CCGAC (Fig. S1B; CRT/DRE no. 2). In the Mf*CAS30* distal conserved block was a second pair of CRT/DRE motifs separated by 40 nucleotides (Supplemental Fig. S1B). The homologous region of Mt*CAS31* shared one of the CRT/DRE motifs, CRT/DRE 4, but the second motif, CRT/DRE 3, was absent due to altered nucleotide residues in two of the five core CRT/DRE positions (Supplemental Fig. S1B). Otherwise, the flanking region was essentially identical (Supplemental Fig. S1B). Further upstream of the Mf*CAS30* CDS were five additional CRT/DRE motifs, four of which formed closely spaced pairs (Supplemental Fig. S1B).

Motif Searches Identify the CRT/DRE

As the *Medicago CAS* genes exhibit similar expression kinetics in response to low temperature as the Arabidopsis *COR*, barley (*Hordeum vulgare*) *DHN5* (dehydrin) and *DHN8*, and wheat (*Triticum aestivum*) *WCS120* (wheat cold-specific) genes, we also searched the upstream regions of these genes for common motifs using the motif finding software tool Weeder (Pavesi et al., 2004). Inputting the upstream region of nine of these sequences along with the four *CAS* gene upstream regions resulted in an output in which different permutations of the CRT/DRE on the sense and antisense strand were the top-scoring motifs (not shown). Different permutations of the ABRE core sequence ACGT were the only other motifs to appear more than once. However, the highest ranking motifs were GTCCCT and CCGACA. Motif searches were carried out with and without the GC-rich monocot sequences; with just the distal and proximal regions of *CAS15*, *CAS30*, and *CAS31*, and also with the non-identical spacer between the distal and proximal element. In each test, the output was altered somewhat, nevertheless the same highest ranking motifs remained GTCCCT and CCGACA. The four distal CRT/DRE motifs in both *CAS15* homologs and CRT/DRE motifs 2 and 3, which were present in Mf*CAS30* but absent from Mt*CAS31* had one of the nucleotide permutations.

Carrying out a similar analysis using only four *Medicago CAS* upstream sequences and only their distal and proximal conserved regions did not identify the CRT/DRE. The five top-scoring motifs resulting from this search were the sequences flanking the TATA box (motif 1 [M1]), a motif in the distal conserved region (M2), the transcriptional start site (M3), a motif near the 5′ end of both proximal conserved regions (M4), and one of the ABRE motifs (M5; Supplemental Fig. S1).

Medicago CAS Gene Expression Is Only Partially Faithfully Reproduced in Arabidopsis

The presence of the clustered CRT/DRE and ABRE motifs in the distal upstream conserved block of *M. truncatula* and *M. falcata CAS15* suggested that this region might function as a regulatory island critical for the low-temperature induction of *CAS15*. To explore this idea we generated Mt*CAS15* promoter constructs that were either inclusive of the CRT/DRE and ABRE motifs (pMC7), or exclusive of these motifs (pMC1), fused the promoter regions to the *uidA* (GUS) reporter gene, and transformed them into Arabidopsis (Fig. 5; Supplemental Fig. S1). Expression analyses indicated that constructs lacking the upstream CRT/DRE and ABRE island were not low-temperature responsive (Fig. 5A). However, constructs harboring the CRT/DRE and ABRE island were also not cold-responsive in either as robust a manner as Arabidopsis *COR15* (Fig. 5A), or as *Medicago CAS15* was in both *Medicago* species (Fig. 2). Of the six independent pMC7 lines generated, only pMC7-6 showed low-temperature responsiveness; the other five lines did not (Fig. 5).

We also asked whether Mt*CAS31*$_{pro}$:*uidA* and Mf*CAS30*$_{pro}$:*uidA* fusions would show cold-responsiveness in Arabidopsis. Fusion constructs were generated such that they included two CRT/DRE motifs and all common ABRE motifs immediately proximal to the CDS. The data from these experiments indicated that both the Mt*CAS31*$_{pro}$:*uidA* and Mf*CAS30*$_{pro}$:*uidA* fusions were cold-responsive but a more robust cold response resulted from a greater proportion of the Mf*CAS30*$_{pro}$:*uidA* transgenic lines than from the Mt*CAS31*$_{pro}$:*uidA* lines (Fig. 5, B and C). Addition of the Mf*CAS30* distal segment harboring the additional pairs of closely spaced CRT/DRE motifs (construct pMC2 + 8; Fig. 5B) to the Mt*CAS31* pMC2 promoter
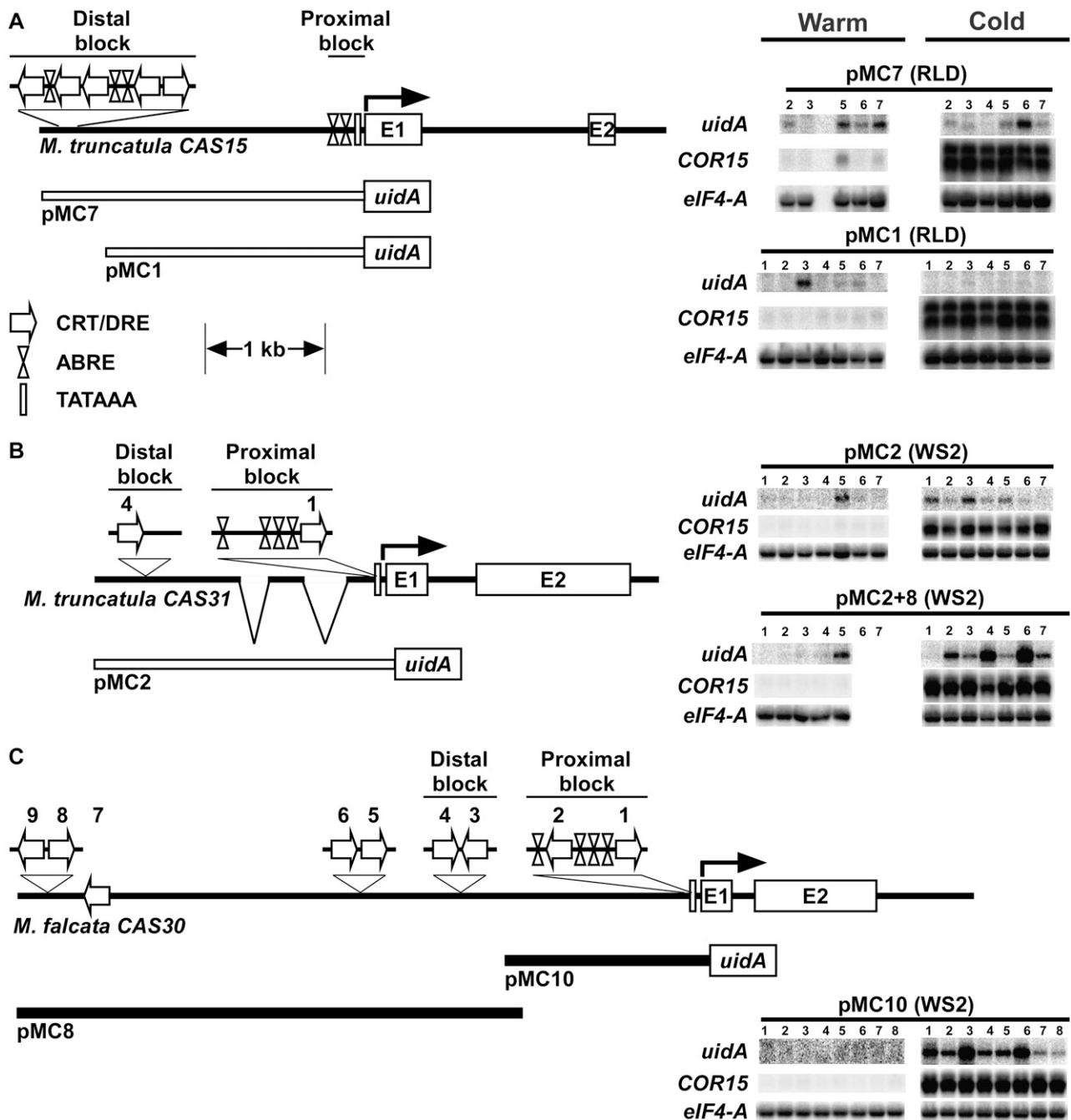
Figure 5. RNA blot analysis of *Medicago CAS* promoter *uidA* fusions in Arabidopsis. A, Mt*CAS15* and the Mt*CAS15* promoter-*uidA* reporter gene fusion constructs that either included (pMC7), or excluded (pMC1) the distal upstream CRT/DRE and ABRE motifs (B) Mt*CAS31* and the Mt*CAS31* promoter-*uidA* reporter gene fusion constructs pMC2 and pMC2+8. C, Mf*CAS30* and the Mf*CAS30* promoter-*uidA* reporter gene fusion construct pMC10. Line drawings are drawn to scale, except for the clustered CRT/DRE and ABRE sequences, which are shown above the scaled horizontal genomic regions. CRT/DRE motifs in the Mf*CAS30* upstream region are numbered beginning with number 1 adjacent to the CDS. The numbering of CRT/DRE motifs in Mt*CAS31* is based on homology with Mf*CAS30* and follows that of the Mf*CAS30* scheme. The two breaks in Mt*CAS31* represent deletions relative to Mf*CAS30*. Expression analysis conducted using T$_2$ plants from multiple independent lines of each construct transformed into Arabidopsis laboratory strain RLD (pMC7 and pMC1) or WS-2 (pMC2, pMC10, and pMC2+8) and assayed for *uidA*, *COR15*, and *eIF4-A* transcript accumulation under noninducing conditions (warm) or after 6 h of low-temperature exposure (cold). Each lane contains 7 μg total RNA.

construct resulted in a greater number of lines exhibiting a robust response to low temperatures (Fig. 5B).

CAS31 Is a Single Gene in *M. truncatula* Whereas Multiple *CAS30*-Like Genes Exist in Diploid *M. falcata*

As the *CAS30* genomic clone encoded a polypeptide substantially larger than that of either the highly identical alfalfa *CAS17* and *CAS18* cDNAs (Wolfraim and Dhindsa, 1993; Wolfraim et al., 1993), we conducted DNA blot hybridization using fragments encompassing different regions of *CAS30* to gain greater insight into the gene family complexity (Fig. 6). DNA Southern-blot hybridizations were conducted using genomic DNAs from the clonally propagated diploid accession PI502449V, the genotype used to construct the genomic library, and a second clonally propagated plant derived from the same *M. falcata* seed accession, PI502449H. Hybridization with an Exon 1 probe produced a pattern consistent with the fragment sizes predicted from the DNA sequences, but there were also several additional cross-hybridizing fragments (Fig. 6, A and B). An additional higher M_r, 18 to 20 kb, *Eco*RI fragment, plus a number of smaller *Eco*RI fragments were also detected (Fig. 6A). *Eco*RV and *Xba*I digests also produced several additional higher M_r, but weaker cross-hybridizing fragments (Fig. 6A).

CAS30 Exon 2 (the *CAS17* homologous region) hybridization resulted in a weak signal in PI502449V at the predicted *Eco*RI and *Eco*RV sized fragments, and instead hybridized much more strongly to fragments that were approximately 5 and 6.6 kb (*Eco*RI) and 23 kb (*Eco*RV), respectively (Fig. 6, A and B). An *Xba*I digest produced the predicted fragment plus an additional higher M_r fragment migrating at approximately 15 to 16 kb (Fig. 6A).

Hybridization of the Mf*CAS30* Exon 1 and Exon 2 fragments to PI502449H genomic DNAs resulted in patterns that were for the most part similar, albeit not identical to those exhibited by PI502449V (Fig. 6A).
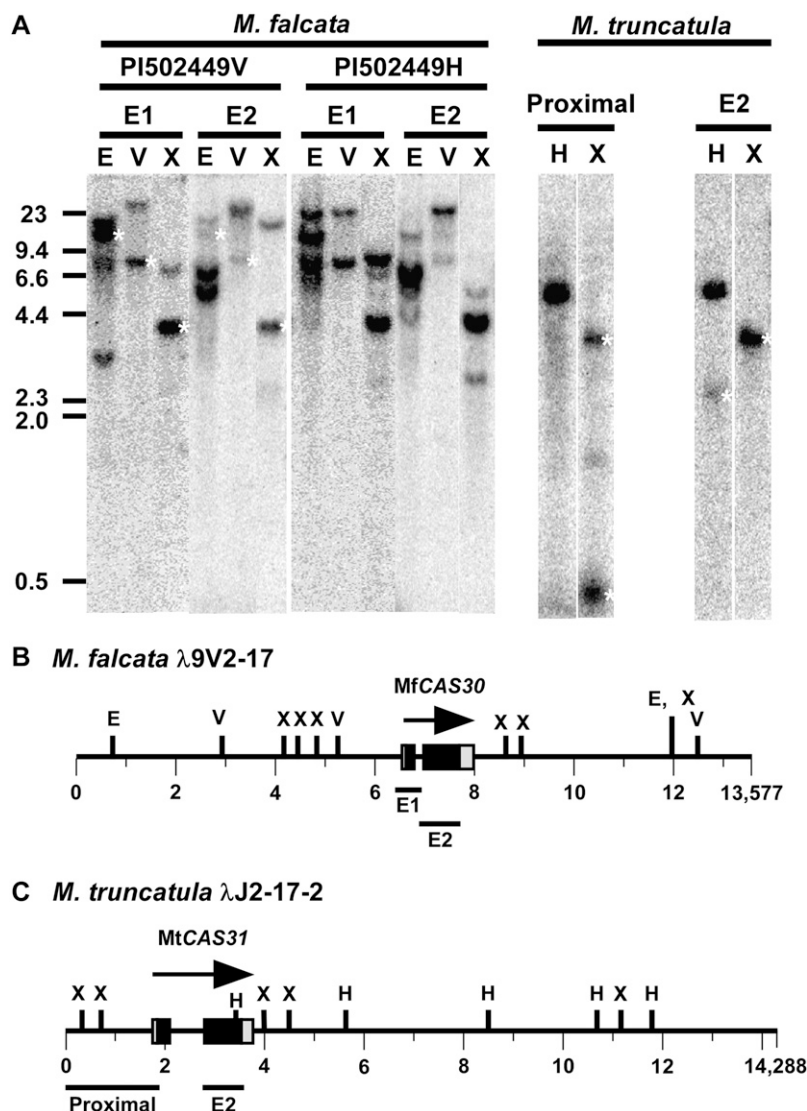
Figure 6. *CAS30* and *CAS31* complexity in *M. falcata* and *M. truncatula*. A, DNA blot analyses of diploid *M. falcata* genotypes PI502449V (9V) and PI502449H (9H), and *M. truncatula* 'Jemalong'. White asterisks identify the fragments predicted from the genomic sequence. B, Structure of the *M. falcata CAS30* genomic region. C, Structure of the *M. truncatula CAS31* genomic region. E1, Exon 1; E2, Exon 2; E, *Eco*RI; V, *Eco*RV; H, *Hin*dIII; X, *Xba*I. Distances in kilobase are indicated below. Fragments used as probes are drawn below the genomic regions.

The pattern produced with *Xba*I digestion and *CAS30* Exon 2 probe resulted in one band shared between PI502449V and PI502449H, but there were additional bands present in PI502449H (Fig. 6A). Similarly, the lower 11 kb *Eco*RI fragment forming the doublet pair in PI502449V with the Exon 1 probe was present in PI502449H, but the higher M_r fragment was not and instead "new" fragments appeared at about 23 and 6.6 kb (Fig. 6A).

Hybridization to *M. truncatula* DNA with the *M. truncatula* *CAS31* proximal-promoter-Exon 1 fragment produced the predicted *Xba*I fragments of 3,269 and 389 bp, and an additional weaker hybridizing fragment approximately 1.5 kb in size (Fig. 6, A and C). (This latter fragment extended beyond the 5' end of our genomic clone.) The 3,269 bp *Xba*I fragment was also produced by hybridization with the Exon 2 region. Similarly, a predicted 2,210 bp *Hin*dIII fragment of weak signal intensity resulted from hybridization with the Exon 2 region, and an approximately 5-kb fragment, which extended beyond the 5' of our genomic clone and was predicted to be at least 3,424 bp in size (Fig. 6, A and C).

Taken together these data indicate that the *M. truncatula* genome harbors only a single *CAS31* gene, whereas the *M. falcata* genome harbors the *CAS30* gene, and at least one additional gene that share the *CAS30* Exon 1 and 2 fragments. Adding to the complexity, a single *M. falcata* accession harbors two allelic forms of these genes.

DISCUSSION

The 5-bp CRT/DRE motif forms the conserved core of a cis-acting regulatory element to which the CBF transcription factors bind (Baker et al., 1994; Yamaguchi-Shinozaki and Shinozaki, 1994; Stockinger et al., 1997; Liu et al., 1998). Multiple copies present in the highly induced cold-responsive genes of many dicot and monocot species suggest the CRT/DRE is a plant-universal cis-acting regulatory element. Expression analyses and alignment of the MfCAS30 and MtCAS31 upstream regions indicate that it is not just the presence of the CRT/DRE, however, but of equal importance is the contextual positioning of the CRT/DRE relative to a second motif. A pair of closely spaced CRT/DRE motifs may be more effective at producing a transcriptional output than two distantly spaced motifs. Mechanistically these paired CRT/DRE motifs may function similar to the binding sites in Notch target genes in which "sequence-paired" binding sites act to fine-tune responsiveness to Notch protein levels (Cave et al., 2005; Nam et al., 2007).

M. truncatula and *M. falcata* also differed in the number of *CAS31*/*CAS30* homologs. *M. truncatula* harbored a single *CAS31* gene whereas the diploid *M. falcata* harbored at least two homologs. Thus tetraploid alfalfa is likely to harbor a minimum of four *CAS30* homologs. The Southern hybridization experiments indicate that there are at least two different genes that possess the MfCAS30 Exon 1 fragment (in addition to each individual possessing two allelic forms of each gene), whereas the northern hybridization experiments suggest two types of genes. One that produces the larger species of transcript recognized by the Exon 1 probe and the second smaller M_r species of transcript recognized by the *CAS17*/Exon 2 probe. Caution must be exercised in equating the signal intensity with gene copy numbers, however, because the Exon 1 probe is unique whereas the *CAS17*/Exon 2 region is of low complexity, and consists of multiple partially repetitive units. In essence *M. falcata* harbors more *CAS31*/*CAS30* homologs, which are more cold-responsive than *M. truncatula*. The greater low-temperature responsiveness appears to be due to greater numbers of paired CRT/DRE motifs in the *M. falcata* *CAS30* promoter. Both of these scenarios were postulated to account for the differences across alfalfa cultivars in which a positive relationship exists between the expression levels of certain *CAS* genes detected in an individual cultivar and the low-temperature tolerance limit of that cultivar (Mohapatra et al., 1989).

CAS15 was a slightly different story from MfCAS30 and MtCAS31. *CAS15* was highly cold-responsive in both *M. truncatula* and *M. falcata*. However, introducing the pMC7 MtCAS15$_{PRO}$:*uidA* fusions harboring the distal CRT/DRE-ABRE island into the Arabidopsis genome did not result in convincing cold-responsiveness. Nonetheless, the pMC1 constructs lacking the CAS15 CRT/DRE island were completely non-cold-responsive. What these data suggest is that although at the nucleotide level the cis-elements are conserved, the promoter architecture may be interpreted differently in Arabidopsis than in *Medicago*. Other regulatory elements crucial in facilitating gene expression may also exist in the *CAS* gene promoters and these may function differently in *Medicago* than in Arabidopsis. Thus, Arabidopsis may not be the best system for functional analyses of these *Medicago* promoters despite the relative ease of recovering transgenic Arabidopsis.

Sequencing the entire bacteriophage λ genomic inserts encompassing the two *Medicago* species *CAS* genes and aligning them also yielded tremendous insight into the *CAS* gene structure. The *CAS* gene upstream regions have maintained blocks of identity separated by regions of sequence diversity. In the case of the *M. falcata* and *M truncatula CAS15* genomic regions, cis-acting regulatory elements critical for low-temperature-induced expression in many other monocot and dicot species, are indeed present in the *CAS15* upstream regions, but they are positioned much farther away from the protein CDSs than might have been expected. Negative regulatory elements also exist in the distal region of the soybean Suc binding protein 2 (*SBP2*) promoter, which act to prevent *SBP2* expression in tissues other than seeds and vegetative organ vascular tissues (Waclawovsky et al., 2006). Whether all *Medicago* promoters or even other plants of the Fabaceae exhibit such a similar architecture, is at

present unknown. Importantly, however, similar alignments of syntenous colinear stretches of genomic regions from human and mouse, and other related taxa show that there are conserved noncoding sequences 10 kb or more distal to the protein CDSs, which may be upstream, downstream or within, even with introns (Adams, 2005; Lockton and Gaut, 2005; Bird et al., 2006). Functional assays show that these regions, or regulatory modules play a critical role in directing gene expression in spatial and temporal dimensions (Davidson, 2006).

A final important point is that morphological and anatomical differences between *M. falcata* and *M. truncatula* are likely to be a contributing factor in the capacity of plants to survive low temperatures. The cold-treated *M. truncatula* crown tissues showed a slightly greater TEL_{50} of $-8°C$ in comparison to the $-4°C$ TEL_{50} of leaves suggesting that the crown has greater capacity for low-temperature tolerance. However, the whole-plant low-temperature tolerance assays were more consistent with the leaf TELs, which may be due to the absence of meristematic cells in the *M. truncatula* crown region capable of generating new shoots and roots. Whereas *M. truncatula* has a clearly defined region that separates a primary shoot apex and meristem from the root, *M. falcata* exhibits a branched structure with multiple stems and a less distinct crown region that consisted of numerous underground stems with lateral buds (Oliver, 1913). In addition, *M. falcata* can produce adventitious buds from roots giving the plant a "creeping rootedness" growth habit (Oakley and Garver, 1913). These growth habits are an important aspect of winter hardiness because the meristematic regions impart the capacity for regrowth after frost heaving, the expansion and contraction of soil during freeze-thaw cycles that literally throws the plant out of the soil (Southworth, 1921; Castonguay et al., 2006). These growth habit forms also differ significantly from afalfa, which has a single large tap root. This difference in growth habit bears pointing out because for much of the 20th century, a central objective of alfalfa-breeding programs was to increase winter hardiness, and the primary source for this trait was *M. falcata* (Quiros and Bauchan, 1988). Introduction of the creeping rootedness growth habit from *M. falcata* into alfalfa followed by genetic analyses indeed shows a high positive correlation between the creeping rootedness growth habit and winter hardiness (Heinrichs and Morley, 1960). What would be particularly exciting is if the CBF response pathway is tied into the capacity for regrowth of meristematic regions.

MATERIALS AND METHODS

Plant Material

Medicago truncatula 'Jemalong' and *Medicago falcata* accessions PI502447 and PI502449 were obtained through the U.S. Department of Agriculture (USDA) GRIN system (http://www.ars-grin.gov/). The USDA *Medicago*

germplasm collection has been rated on a numerical scale of 1 to 10 for numerous traits of agronomic value including frost and winter injury damage. Both accessions PI502447 and PI502449 were ranked as the most resistant to winter injury (USDA rating no. 1) and have been karyotyped as diploid alfalfa (*Medicago sativa*) subsp. *falcata* (Brummer et al., 1999). Accession PI502447 is of "wild" origin and accession PI502449 is a Russian cultivar known as 'Severyanka' originally obtained by the USDA from the N.I. Vavilov Institute of Plant Industry, St. Petersburg, Russia. *M. truncatula* 'Jemalong' seed was soaked in concentrated sulfuric acid for 10 min, rinsed three times with distilled H_2O, and germinated on moistened filter paper. Approximately 15 seedlings of each genotype were transplanted to 1-gallon pots and placed into the greenhouse where the individual plants continued to grow. The 'Jemalong' plants displayed morphological variation: a pronounced maroon splotch was noted in most but not all individuals. To obtain a more uniform genotype and inbred homozygous line, we selected one individual displaying the pronounced maroon splotch and performed single seed descent for two generations. To work with a less heterogeneous *M. falcata* population, we selected two individual plants and clonally propagated these individuals by cuttings. These individuals were selected based on a clear phenotypic difference displayed in both *M. falcata* populations. This phenotype was either a more horizontal growth habit, or a pronounced vertical growth habit; and the clonally propagated individuals were deemed accordingly: PI502447H, PI502447V, PI502449H, and PI502449V. No connection between growth habit and other traits were assumed. The resulting single seed descent 'Jemalong' and clonally propagated *M. falcata* material were then used for the low-temperature tolerance assays, the bacteriophage λ genomic libraries, and all DNA and RNA blot analyses.

Low-Temperature Tolerance Assays

Four-week-old clonally propagated *M. falcata* plants and 4-week-old *M. truncatula* seedlings were used to evaluate low-temperature tolerance. Plants were grown in Bacto Promix (Michigan Peat Company) under a 16-h photoperiod at a light intensity of 250 μmol m^{-2} s^{-1} photosynthetically active radiation provided by cool-white fluorescent lamps using a 20°C/18°C day/night regime. Only healthy well-watered plants fertilized once a week with 0.5 g L^{-1} of an all purpose 20:20:20 plant nutrient solution (Schultz) were used. Plants of each species were divided into two groups. Plants in one group were used to measure low-temperature tolerance without cold-acclimating conditions, and were maintained in an environmentally controlled chamber under the conditions described above. Plants in the second group were transferred to a growth chamber set at constant 2°C with a 12-h photoperiod under 150 μmol m^{-2} s^{-1} photosynthetically active radiation for 4 weeks.

Low-temperature tolerance of nonacclimated and acclimated plants of *M. falcata* and *M. truncatula* was determined on detached leaf discs and crown segments by electrolyte leakage (Pennycooke et al., 2003) and by regrowth (Dhont et al., 2002). Three leaf discs (5 mm in diameter) and crowns (8 mm above the apex) were placed in 50-mL conical tubes, respectively. Three tubes of each treatment were used for each test temperature. Runs were conducted by placing tubes in a programmable freezer (Tenney/Lunaire). The tubes were maintained at 0°C for 1 h after which a small chip of ice was placed in contact with the plant tissue in each tube. Following ice nucleation, the samples were allowed to equilibrate for an additional hour and the temperature was decreased at a rate of 2°C h^{-1} to various temperatures (lowest temperature $-20°C$); each temperature was then held constant for 30 min. Test temperatures were confirmed by thermocouple readings. Tubes were then removed and placed in a growth chamber at 2°C to thaw overnight. Approximately 25 mL deionized, distilled water was added to each tube, and the tubes were shaken for 1 h at 250 rpm before reading the conductivity (C_1) with an accumet Basic AB30 electrical conductivity meter (Fisher Scientific). Tubes were then frozen for a minimum of 1 h at $-80°C$, thawed, and shaken before measuring the total potential conductivity (C_2). Relative TEL represents the mean ion leakage as a percentage of the total leakage from frozen-killed samples (C_1/C_2) $\times$ 100. Three sets of data points were generated for each temperature point of the run, with three tubes representing each data point.

Whole plants were treated and frozen as described above for detached leaves and crowns with the following modifications. Styrofoam chips were added to the pots to simulate snow cover during an artificial freeze (C. Stushnoff, personal communication), plants were misted with tap water at 0°C to initiate extracellular ice nucleation, and then allowed to equilibrate at $-3°C$ for 15 h before further temperature decreases. Whole plants were thawed slowly at 2°C overnight and returned to growth chambers to regrow under the initial establishment conditions described above. Shoots were

harvested after a 3-week regrowth period and oven dried at 60°C for dry-weight determination. Regrowth was expressed as a percentage of the non-frozen control. Three plants per pot and five pots per treatment were used for each test temperature. The temperature (TEL_{50}) that resulted in either 50% ion leakage (calculated using a fitted model plot), or 50% kill as indicated by lack of regrowth was defined as the LT_{50}. These experiments were repeated twice. Statistical analyses were performed with statistical software (SAS).

Treatment of Plant Material Used for Low-Temperature Experiments

'Jemalong' seed was germinated as described above. One to three seedlings per 4-inch pot were transplanted into high-porosity soilless mix (Bacto). Pots were set inside trays and the trays placed into a BD16 growth chamber (Conviron) under combined metal halide and high-pressure sodium lamps at a light intensity of 500 μmol m^{-2}s^{-1}. Growth conditions were 17 h light, 7 h dark cycle, constant 25°C, and 60% relative humidity for approximately 3 weeks prior to the temperature drop at the indicated times (details in Fig. 2 legend). Vigorous, bushy greenhouse-grown *M. falcata* plants were cut back to approximately 5 to 8 cm above the soil and placed into the growth chamber concurrently with the transplanted 'Jemalong' seedlings. At the time of the temperature drop, the light intensity was simultaneously reduced to approximately 225 μmol m^{-2}s^{-1}. Plants were deacclimated by returning the chamber to 25°C and the original light intensity.

T_2 seeds of the *Medicago CAS* promoter-*uidA* fusion constructs in the Arabidopsis ecotype backgrounds RLD and WS-2 (pMC) were surfaced sterilized in 30% bleach and 0.2% Triton X-100 for approximately 20 min followed by four washes in sterile water. The seeds were stratified at 4°C for 4 d. Seeds were sown on Gamborg's B5 (GibcoBRL Life Technologies) plates containing 0.8% (w/v) phytagar and 2% Suc and incubated at 22°C with a 16-/8-h photoperiod under cool-white fluorescent light at 100 μmol m^{-2} s^{-1}. Four weeks after germination, seven or eight lines of each construct were transferred to a 4°C cold room or maintained at room temperature for 6 h.

PCR Amplification of the *Medicago CBF, CAS,* and *eIF4-a* Genes

To identify *CBF* sequence homologs from *Medicago* we performed a BLAST search of the *M. truncatula* database (Lamblin et al., 2003) maintained on the TIGR Web site server (http://www.tigr.org/) using the Arabidopsis CBF1 sequence as a query. Three distinct sequences or sequence assemblies, TC41456, EST457811, and TC41639 were identified that harbored the CBF signature sequence, and were PCR amplified from genomic DNA. We deemed these Mt*CBF1* (GenBank accession EU139866), Mt*CBF2* (GenBank accession EU139867), and Mt*CBF3* (GenBank accession EU139868), which reflected chronological identification, and not orthology to Arabidopsis *CBF1, CBF2,* and *CBF3*. Our initial *CAS15* clone was PCR amplified from *M. truncatula* 'Jemalong' DNA with primers 5'-ATGGCTGGAATCATGAACAA-3' and 5'-TAACAAAGCA-GTGGGGGTTT-3' using TC8441 as the target, which was the highest scoring *M. truncatula* hit (score 482, e^{-133}) to *M. falcata CAS15*. The initial *CAS17* clone was PCR amplified from *M. sativa* subsp. *falcata* PI502449V genomic DNA using primers 5'-CTGGAACTGGAACAGGTCGT-3' and 5'-TGCCCCTAC-ACTAAAATTCAA-3'. The eIF-4a clone, based on TC51169, the highest scoring BLAST hit (score 605, e^{-169}) to tobacco eIF4A1 (Owttrim et al., 1994), was amplified from *M. truncatula* genomic DNA using primers 5'-TTGCAG-CAGCTTGATTATGG-3' and 5'-CTTGTCAGTGAGCCAGTCCA-3'. All PCR products were cloned into the vector pGEM-T-Easy (Promega) and sequenced at The Ohio State University/Ohio Agricultural Research and Development Center, Molecular and Cellular Imaging Center to confirm their identity.

Bacteriophage λ Genomic Library Constructions; Screening and Sequencing of Inserts

High M_r total plant genomic DNA, isolated as described (Stockinger et al., 1996), was partially restricted with *Sau*3AI and used for ligation to bacteriophage λ vector λ Fix II using the components of the λ FixII Gigapack III XL kits and following the manufacturer's recommendations (Stratagene). Plaque-purified bacteriophage λ genomic clones cross-hybridizing with Mf*CAS17* and Mt*CAS15* were subcloned into the *Not*I site of plasmid vector pGEM-11Zf(−) (Promega), which was used to prepare shotgun subclone libraries for DNA sequence determination. Detailed procedures for all of the above are available on the Stockinger Lab Web site (http://www.oardc.ohio-state.edu/

stockingerlab/). Shotgun sequence assembly utilized the software package Sequencher (Gene Codes).

Genomic clones cross-hybridizing with Mt*CAS15* and Mf*CAS17* PCR-amplified products selected for DNA sequence determination included, Mt*CAS15*: λJ4-15-1/GenBank accession EU139869; Mf*CAS15*: λ7H-15-2/Gen-Bank accession EU139870; Mt*CAS31*: λJ2-17 to 2/GenBank accession EU139871; Mf*CAS30*: λ9V-2-17/GenBank accession EU139865.

Annotation of Genomic Sequences

Both the *M. truncatula* and the *M. falcata CAS15* genomic clones were truncated within the CAS15 coding region; λJ4-15-1 truncated in the middle of Intron 1 and λ7H-15-2 truncated at CDS nucleotide 82 (amino acid residue 27). BLAST searches identified the *M. truncatula* BAC clone mth2-15c20 (GenBank accession AC126009) encompassing the remainder of *M. truncatula CAS15* genomic sequence, which was used as the source to complete annotation of Intron 1 and Exon 2. No genomic sequence encompassing the Mf*CAS15* CDS was identified, although BLAST searches identified GenBank accession DQ397199, which encompassed the alfalfa *CAR1* upstream region, and extended to −1,028 relative to the Mf*CAS15* upstream region (not shown). The *M. truncatula CAS15* genomic region was aligned with tentative consensus sequence TC76537 (and TC8441) derived from multiple ESTs. This alignment indicated that the mature mRNA transcript was derived from two exons, but that the protein-encoding region was contained entirely within Exon 1. No genomic sequence encompassing Mf*CAS31* was identified in database collections of *M. truncatula* sequences. To annotate the *M. truncatula* and *M. falcata* genomic sequences isolated with the *M. falcata CAS17* probe, we used the gene structure prediction software GENSCAN (Burge and Karlin, 1997) and comparative alignments with expressed sequences. Both *M. truncatula* (λJ2-17-2) and *M. falcata* (λ9V2-17) genomic regions were scanned for open reading frames using GENSCAN with the Arabidopsis matrix function. The resulting λJ2-17-2 GENSCAN output was a 312-amino-acid CDS predicted to encode a polypeptide of 31,000 M_r. This GENSCAN output was 100% identical to the *M. truncatula* tentative consensus sequence TC100921 (data not shown) indicating that this was probably the bona fide CDS. Alignment of the λJ2-17-2 GENSCAN CDS output and TC100921 to the genomic sequence indicated that the CDS and the entire protein-encoding region were derived from two exons, separated by a single intron. Alignment of the λ9V2-17 GENSCAN output with the *CAS17* cDNA (Wolfraim and Dhindsa, 1993) indicated that the 5' end of Mf*CAS17* resided within Exon 2.

RNA Extraction and Blot Analyses

Total RNA was extracted from Arabidopsis plants using the RNeasy Mini Kit (QIAGEN). Five or 7 μg (as indicated in the figure legends) of total RNA was loaded onto each lane. Fractionation and northern transfers to Hybond-N+ (Amersham Biosciences) were performed as described (Ausubel et al., 1993) except that the transfers were made using 10× sodium citrate. Hybridizations were in 50% formamide, 5× sodium citrate, 20 mM sodium phosphate (pH 6.8), 1× Denhardt's, 0.1% SDS, 10% dextran sulfate, and 100 μg herring sperm DNA. Moderate stringency washes were in 0.2× sodium citrate, 0.05% SDS, and 0.01% sodium pyrophosphate. DNA probes were radiolabeled with ^{32}P-nucleotides, either by random priming or directed priming using SP6 or T7 primers (Feinberg and Vogelstein, 1983) and were visualized by phosphor-image autoradiography using a Storm 860 PhosphorImager (Molecular Dynamics).

Generation of *CAS* Promoter-*uidA* Fusions

Primers were designed to amplify the *CAS* upstream regions (5' end sites along with the 3' end site of pMC2 + 8 are indicated in Supplemental Fig. S1, A and B). Downstream reverse primers were generated within the CDSs of each *CAS* gene resulting in a translational fusion between each *CAS* promoter and *uidA*. Plasmids pMC1 and pMC7 encode the first 25 amino acid residues of Mt*CAS15*; pMC10 encodes the first 18 amino acid residues of Mf*CAS30*; and pMC2 encodes the first 19 amino acid residues of Mt*CAS31*. Amplified products were then subcloned into either pGEM-T-EASY, pGEM-T (Promega), or pUC119. The resulting cloned PCR products were sequenced and subcloned into the *Bam*HI site of pRD420 (Jefferson et al., 1987; Datla et al., 1992). Fusion constructs were electroporated into *Agrobacterium tumefaciens* strain GV3101 (Csaba and Schell, 1986) and transformed into Arabidopsis lab strains RLD and WS-2 via floral dip (Clough and Bent, 1998).

Sequence Manipulation Tools

Percent identity plots (PIPs) were generated using the web interface of the PipMaker (Schwartz et al., 2000). Alignments of CBF and CAS polypeptides were made using the ClustalX windows interface version of ClustalW (Thompson et al., 1997) and were formatted using BOXSHADE 3.2 (http://www.ch.embnet.org/software/BOX_form.html). *CAS* gene upstream nucleotide sequences were aligned using ClustalX in combination with GeneDoc (Nicholas et al., 1997), and formatted using BOXSHADE 3.2. The motif search used the web interface of Weeder (Pavesi et al., 2004). Inputs for the motif searches included the upstream regions of Arabidopsis *COR15a*, *COR15b*, *COR47*, *KIN1*, *COR6.6*, *RD29A*, and *RD29B*; barley (*Hordeum vulgare*) *DHN5* and *DHN8*; and wheat (*Triticum aestivum*) *COR15* (GenBank accession AB095006), and *WCS120* (individual references for each of these sequences, except wheat *COR15*) are provided in Stockinger et al. (2006). Motif searches used the Arabidopsis genome as the reference sequence.

Sequence data from this article can be found in the GenBank/EMBL data libraries under accession numbers EU139865 to EU139871.

Supplemental Data

The following materials are available in the online version of this article.

Supplemental Figure S1. Alignment of the *M. falcata* and *M. truncatula* *CAS* upstream genomic regions.

LITERATURE CITED

Adams MD (2005) Conserved sequences and the evolution of gene regulatory signals. Curr Opin Genet Dev 15: 628–633

Ausubel FM, Brent R, Kingston RE, Moore DD, Seidmen JG, Smith JA, Struhl K (1993) Current Protocols in Molecular Biology. Greene Publishing Associates/John Wiley and Sons, New York

Baker SS, Wilhelm KS, Thomashow MF (1994) The 5′-region of *Arabidopsis thaliana cor15a* has *cis*-acting elements that confer cold-, drought- and ABA-regulated gene expression. Plant Mol Biol 24: 701–713

Barker DG, Bianchi S, Blondon F, Dattée Y, Duc G, Essad S, Flament P, Gallusci P, Génier G, Guy P, et al (1990) *Medicago truncatula*, a model plant for studying the molecular genetics of the Rhizobium-legume symbiosis. Plant Mol Biol Rep 8: 40–49

Bell CJ, Dixon RA, Farmer AD, Flores R, Inman J, Gonzales RA, Harrison MJ, Paiva NL, Scott AD, Weller JW, et al (2001) The Medicago Genome Initiative: a model legume database. Nucleic Acids Res 29: 114–117

Bird CP, Stranger BE, Dermitzakis ET (2006) Functional variation and evolution of non-coding DNA. Curr Opin Genet Dev 16: 559–564

Brummer EC, Cazcarro PM, Luth D (1999) Ploidy determination of alfalfa germplasm accessions using flow cytometry. Crop Sci 39: 1202–1207

Burge C, Karlin S (1997) Prediction of complete gene structures in human genomic DNA. J Mol Biol 268: 78–94

Castonguay Y, Laberge S, Brummer EC, Volenec JJ (2006) Alfalfa winter hardiness: a research retrospective and integrated perspective. Adv Agron 90: 203–265

Cave JW, Loh F, Surpris JW, Xia L, Caudy MA (2005) A DNA transcription code for cell-specific gene activation by notch signaling. Curr Biol 15: 94–104

Chinnusamy V, Ohta M, Kanrar S, Lee BH, Hong X, Agarwal M, Zhu JK (2003) ICE1: a regulator of cold-induced transcriptome and freezing tolerance in Arabidopsis. Genes Dev 17: 1043–1054

Close TJ (1996) Dehydrins: emergence of a biochemical role of a family of plant dehydration proteins. Physiol Plant 97: 795–803

Clough SJ, Bent AF (1998) Floral dip: a simplified method for Agrobacterium-mediated transformation of *Arabidopsis thaliana.* Plant J 16: 735–743

Cook DR (1999) *Medicago truncatula*—a model in the making! Curr Opin Plant Biol 2: 301–304

Csaba K, Schell J (1986) The promoter of TL-DNA gene 5 controls the tissue-specific expression of chimaeric genes carried by a novel type of *Agrobacterium* binary vector. Mol Gen Genet 204: 383–396

Datla RS, Hammerlindl JK, Panchuk B, Pelcher LE, Keller W (1992) Modified binary plant transformation vectors with the wild-type gene encoding NPTII. Gene 122: 383–384

Davidson EH (2006) The Regulatory Genome: Gene Regulatory Networks in Development and Evolution. Elsevier/Academic Press, Amsterdam

Dhont C, Castonguay Y, Nadeau P, Belanger G, Chalifour FP (2002) Alfalfa root carbohydrates and regrowth potential in response to fall harvests. Crop Sci 42: 754–765

Feinberg AP, Vogelstein B (1983) A technique for radiolabeling DNA restriction endonuclease fragments to high specific activity. Anal Biochem 132: 6–13

Fowler S, Thomashow MF (2002) *Arabidopsis* transcriptome profiling indicates that multiple regulatory pathways are activated during cold acclimation in addition to the CBF cold response pathway. Plant Cell 14: 1675–1690

Gilmour SJ, Zarka DG, Stockinger EJ, Salazar MP, Houghton JM, Thomashow MF (1998) Low temperature regulation of the Arabidopsis CBF family of AP2 transcriptional activators as an early step in cold-induced *COR* gene expression. Plant J 16: 433–442

Haagenson DM, Cunningham SM, Joern BC, Volenec JJ (2003) Autumn defoliation effects on alfalfa winter survival, root physiology, and gene expression. Crop Sci 43: 1340–1348

Heinrichs DH, Morley FHW (1960) Inheritance of resistance to winter injury and its correlation with creeping rootedness in alfalfa. Can J Plant Sci 40: 487–489

Ivashuta S, Uchiyama K, Gau M, Shimamoto Y (2002) Linear amplification coupled with controlled extension as a means of probe amplification in a cDNA array and gene expression analysis during cold acclimation in alfalfa (*Medicago sativa* L.). J Exp Bot 53: 351–359

Iwasaki T, Kiyosue T, Yamaguchi-Shinozaki K, Shinozaki K (1997) The electronic plant gene register: the dehydration-inducible *Rd17* (*Cor47*) gene and its promoter region in *Arabidopsis thaliana* (accession no. AB004872). Plant Physiol 115: 1287–1289

Jaglo-Ottosen KR, Gilmour SJ, Zarka DG, Schabenberger O, Thomashow MF (1998) Arabidopsis *CBF1* overexpression induces *COR* genes and enhances freezing tolerance. Science 280: 104–106

Jaglo KR, Kleff S, Amundsen KL, Zhang X, Haake V, Zhang JZ, Deits T, Thomashow MF (2001) Components of the Arabidopsis C-repeat/dehydration-responsive element binding factor cold-response pathway are conserved in *Brassica napus* and other plant species. Plant Physiol 127: 910–917

Jefferson RA, Kavanagh TA, Bevan MW (1987) GUS fusions: beta-glucuronidase as a sensitive and versatile gene fusion marker in higher plants. EMBO J 6: 3901–3907

Jones JS, Bingham ET (1995) Inbreeding depression in alfalfa and cross-pollinated crops. Plant Breed Rev 13: 209–233

Lamblin AF, Crow JA, Johnson JE, Silverstein KA, Kunau TM, Kilian A, Benz D, Stromvik M, Endre G, VandenBosch KA, et al (2003) MtDB: a database for personalized data mining of the model legume *Medicago truncatula* transcriptome. Nucleic Acids Res 31: 196–201

Lesins KA, Lesins I (1979) Genus Medicago (Leguminosae). A Taxogenetic Study. Dr. W. Junk Publishers, The Hague, The Netherlands

Liu Q, Kasuga M, Sakuma Y, Abe H, Miura S, Yamaguchi-Shinozaki K, Shinozaki K (1998) Two transcription factors, DREB1 and DREB2, with an EREBP/AP2 DNA binding domain separate two cellular signal transduction pathways in drought- and low-temperature-responsive gene expression, respectively, in *Arabidopsis*. Plant Cell 10: 1391–1406

Lockton S, Gaut BS (2005) Plant conserved non-coding sequences and paralogue evolution. Trends Genet 21: 60–65

Mohapatra SS, Wolfraim L, Poole RJ, Dhindsa RS (1989) Molecular cloning and relationship to freezing tolerance of cold-acclimation-specific genes of alfalfa. Plant Physiol 89: 375–380

Monroy AF, Castonguay Y, Laberge S, Sarhan F, Vezina LP, Dhindsa RS (1993) A new cold-induced alfalfa gene is associated with enhanced hardening at subzero temperature. Plant Physiol 102: 873–879

Nam Y, Sliz P, Pear WS, Aster JC, Blacklow SC (2007) Cooperative assembly of higher-order Notch complexes functions as a switch to induce transcription. Proc Natl Acad Sci USA **104:** 2103–2108

Nam YW, Penmetsa RV, Endre G, Uribe P, Kim D, Cook DR (1999) Construction of a bacterial artificial chromosome library of *Medicago truncatula* and identification of clones containing ethylene-response genes. Theor Appl Genet **98:** 638–646

Nicholas KB, Nicholas HB Jr, Deerfield DW II (1997) GeneDoc: analysis and visualization of genetic variation. EMBNET NEWS **4:** 1–4

Oakley RA, Garver S (1913) Two types of proliferation in alfalfa. US Dept Agr Bur Plant Ind Circ **115:** 1–51

Oliver GW (1913) Some new alfalfa varieties for pasture. US Dept Agr Bur Plant Ind Bull **258:** 1–13

Owttrim GW, Mandel T, Trachsel H, Thomas AA, Kuhlemeier C (1994) Characterization of the tobacco eIF-4A gene family. Plant Mol Biol **26:** 1747–1757

Pavesi G, Mereghetti P, Mauri G, Pesole G (2004) Weeder Web: discovery of transcription factor binding sites in a set of sequences from co-regulated genes. Nucleic Acids Res **32:** W199–203

Penmetsa RV, Cook DR (2000) Production and characterization of diverse developmental mutants of *Medicago truncatula.* Plant Physiol **123:** 1387–1398

Pennycooke JC, Jones ML, Stushnoff C (2003) Down-regulating alpha-galactosidase enhances freezing tolerance in transgenic petunia. Plant Physiol **133:** 901–909

Quiros CF, Bauchan GR (1988) The genus *Medicago* and the origin of the *Medicago sativa* complex. *In* AA Hanson, DK Barnes, RR Hill Jr, eds, Alfalfa and Alfalfa Improvement. American Society of Agronomy, Madison, WI, pp 93–124

Schwartz S, Zhang Z, Frazer KA, Smit A, Riemer C, Bouck J, Gibbs R, Hardison R, Miller W (2000) PipMaker—a web server for aligning two genomic DNA sequences. Genome Res **10:** 577–586

Small E, Jomphe M (1989) A synopsis of the genus Medicago (Leguminosae). Can J Bot **67:** 3260–3294

Southworth W (1921) A study of the influence of the root system in promoting hardiness in alfalfa. Sci Agric **1:** 5–9

Stockinger EJ, Cheng H, Skinner JS (2006) Structural organization of barley *CBF* genes coincident with QTLs for cold hardiness. *In* THH Chen, M Uemura, S Fujikawa, eds, Cold Hardiness in Plants: Molecular Genetics, Cell Biology and Physiology. CABI Publishing Oxon, UK, pp 53–63

Stockinger EJ, Gilmour SJ, Thomashow MF (1997) *Arabidopsis thaliana CBF1* encodes an AP2 domain-containing transcriptional activator that binds to the C-repeat/DRE, a *cis*-acting DNA regulatory element that stimulates transcription in response to low temperature and water deficit. Proc Natl Acad Sci USA **94:** 1035–1040

Stockinger EJ, Mulinix CA, Long CM, Brettin TS, Iezzoni AF (1996) A linkage map of sweet cherry based on RAPD analysis of a microspore-derived callus culture population. J Hered **87:** 214–218

Thomashow MF (1990) Molecular genetics of cold acclimation in higher plants. Adv Genet **28:** 99–131

Thomashow MF (1999) Plant cold acclimation: freezing tolerance genes and regulatory mechanisms. Annu Rev Plant Physiol Plant Mol Biol **50:** 571–599

Thompson JD, Gibson TJ, Plewniak F, Jeanmougin F, Higgins DG (1997) The CLUSTAL_X windows interface: flexible strategies for multiple sequence alignment aided by quality analysis tools. Nucleic Acids Res **25:** 4876–4882

Vogel JT, Zarka DG, Van Buskirk HA, Fowler SG, Thomashow MF (2005) Roles of the CBF2 and ZAT12 transcription factors in configuring the low temperature transcriptome of Arabidopsis. Plant J **41:** 195–211

Waclawovsky AJ, Freitas RL, Rocha CS, Contim LA, Fontes EP (2006) Combinatorial regulation modules on GmSBP2 promoter: a distal cis-regulatory domain confines the SBP2 promoter activity to the vascular tissue in vegetative organs. Biochim Biophys Acta **1759:** 89–98

Wang H, Datla R, Georges F, Loewen M, Cutler AJ (1995) Promoters from *kin1* and *cor6.6*, two homologous *Arabidopsis thaliana* genes: transcriptional regulation and gene expression induced by low temperature, ABA, osmoticum and dehydration. Plant Mol Biol **28:** 605–617

Wolfraim LA, Dhindsa RS (1993) Cloning and sequencing of the cDNA for *cas17*, a cold acclimation-specific gene of alfalfa. Plant Physiol **103:** 667–668

Wolfraim LA, Langis R, Tyson H, Dhindsa RS (1993) cDNA sequence, expression, and transcript stability of a cold acclimation-specific gene, *cas18*, of alfalfa (*Medicago falcata*) cells. Plant Physiol **101:** 1275–1282

Yamaguchi-Shinozaki K, Shinozaki K (1994) A novel *cis*-acting element in an *Arabidopsis* gene is involved in responsiveness to drought, low-temperature, or high-salt stress. Plant Cell **6:** 251–264

Young ND, Cannon SB, Sato S, Kim D, Cook DR, Town CD, Roe BA, Tabata S (2005) Sequencing the genespaces of *Medicago truncatula* and *Lotus japonicus*. Plant Physiol **137:** 1174–1181

Zarka DG, Vogel JT, Cook D, Thomashow MF (2003) Cold induction of Arabidopsis *CBF* genes involves multiple ICE (inducer of CBF expression) promoter elements and a cold-regulatory circuit that is desensitized by low temperature. Plant Physiol **133:** 910–918

Zhang X, Fowler SG, Cheng H, Lou Y, Rhee SY, Stockinger EJ, Thomashow MF (2004) Freezing-sensitive tomato has a functional CBF cold response pathway, but a CBF regulon that differs from that of freezing-tolerant Arabidopsis. Plant J **39:** 905–919